Sustainable Food Technology

ROYAL SOCIETY OF CHEMISTRY

PAPER

View Article Online
View Journal | View Issue

Cite this: *Sustainable Food Technol.*, 2025, **3**, 204

Optimization of ultrasonic-assisted extraction of dietary fiber from bhimkol (*Musa balbisiana*) peel using central composite design: physicochemical, functional, and thermal properties

Laxmi Kant Rawat and Tabli Ghosh *

Bhimkol is a seeded banana found in northeastern and southern India, and its peel is a good source of dietary fiber (DF) and can be utilized for various food applications. Considering this, in this study, the optimization of ultrasonic-assisted extraction (UAE) of bhimkol (*Musa balbisiana*) peel powder (BPP)-based DF was carried out. Proximate analysis of the prepared BPP was performed for factors such as moisture (1.40%), fat (2.22%), protein (7.30%), crude fiber (23.39%), and ash (10.47%) content as well as physicochemical, hydration, and thermal properties. The optimization of UAE of DF was carried out considering three independent variables, namely, processing time (20 to 60 min), solvent-to-solid ratio (30 to 70 mL g^{-1}), temperature (40 to 80 °C), and one dependent variable, *viz.* yield (%). The highest extraction yield of DF (49.58 ± 0.88%) was obtained from UAE at a time, solvent/solid ratio, and temperature of 60 min, 30 mL g^{-1}, and 40 °C, respectively. The UAE of DF at optimized conditions was compared to the hot water extraction method (HEM). The obtained DF from BPP under optimized conditions of UAE and HEM was analyzed and compared for physicochemical properties, functional properties and thermal properties. In the food sector, DF can be possibly used in processed food, bakery products, and dairy products for improving food quality and properties.

Received 29th July 2024
Accepted 10th October 2024

DOI: 10.1039/d4fb00230j

rsc.li/susfoodtech

Sustainability spotlight

Bhimkol peel can be transformed into valuable resources, thus reducing environmental impact and promoting sustainability by creating eco-friendly products such as food products and packaging materials. Bhimkol peel is a good source of dietary fibre, which can be extracted using green technologies. Ultrasonic-assisted extraction technique can enhance the quantity and quality of dietary fibre obtained from plant-based sources. Ultrasonic extraction is more effective and faster than conventional techniques, utilizing less chemicals and time. This green approach assists the development and comparison of dietary fibre obtained from waste for sustainable food technologies.

Introduction

Bhimkol (*Musa balbisiana*) belongs to the Musaceae family, which is native to the eastern South region and northern southeast region of Asia;[1] its domestication started approximately 7000 years ago in southeast Asia.[2] Bhimkol is a famous variety of banana in northeast India and is abundant in nutrients such as proteins, fats, carbohydrates (dietary fiber) and micronutrients such as Mg, Zn, K, Se, and amino acids.[3] Thus, being a rich source of minerals, it is widely used for developing functional foods.

Dietary fiber (DF) is classified based on its water solubility into insoluble dietary fiber (IDF) and soluble dietary fiber (SDF). IDF includes cellulose, hemicellulose and lignin, while SDF comprises pectin, mucilage and β-glucans.[4,5] The structure and composition of DF include oligosaccharides and polysaccharides such as cellulose, hemicellulose, resistant starch, gums, pectin, waxes, lignin, mucilage, and glucans, which may have great physiological effects on humans.[6] However, although DF may be partially or fully fermented in the large intestine, it remains resistant to absorption and digestion in the small intestine.[7] DF has various health beneficial properties; for instance, it improves gut health, reduces blood cholesterol, reduces the risk of obesity, reduces the risk of cardiovascular disease, controls blood sugar, and reduces constipation.[4,8–13]

The essential nutrient DF is widely obtained from fruits and vegetables, oat bran, barley bran, wheat bran, cereals, and nuts.[14,15] However, considerable loss may occur during the pre- and post-harvest processing of various food items. DF is also extracted from the fruit, vegetable, and agriculture waste such as papaya peel, kiwifruit, lemon seeds, orange seeds, grapefruit seeds, coconut flour, potato residue, okara, and mango

Department of Food Engineering and Technology, School of Engineering, Tezpur University, Assam, 784028, India. E-mail: tablighosh1@gmail.com

peel.[4,5,12,16–19] Fruit, vegetable and agricultural wastes consist of fats, proteins, SDF, IDF, and other components.[14,20] Thus, the above-mentioned sources can be used to extract various types of DF.

Many different methods can be used to extract DF, including drying, chemical methods, enzymatic methods, ultrasound-assisted extraction, microwave-assisted extraction, high hydrostatic pressure, and subcritical water extraction.[18,19,21,22] Ultrasonic-assisted extraction (UAE) is a potent method for separating bioactive substances from different plant sources. UAE uses high-frequency sound waves to enhance the extraction process and provide significant yields that are effective.[19] Phytochemicals such as polyphenols, vitamins, and polysaccharides are examples of bioactive compounds. Because ultrasonic irradiation greatly improves mass transfer processes, thus, it is a recommended technique for producing high-quality extracts.[23,24] UAE has been previously used to extract DF from various sources such as soybean residues,[25] papaya peel,[12] defatted coconut flour,[19] banana bracts,[13] and mango peel.[19] DF is used in several food products, cosmetic, and pharmaceutical sector. Additionally, it can improve the taste of food products such as meatballs, baked goods, pasta, and ice cream.[26–29]

Based on the above discussion, the current study focused on optimizing the processing condition of DF obtained from BPP using the UAE method based on the yield. Additionally, the UAE method DF extraction was compared with the hot water bath extraction method (HEM). In order to ensure the highest yield of DF, the amounts of the preparation factors were optimized using central composite design (CCD). The properties of DF were compared based on the structural and morphological characteristics and physical properties (bulk density, tapped density, angle of repose, and density). Additionally, the physicochemical properties of DF such as WHC (water holding capacity), OHC (oil holding capacity), and thermal properties and GAC (glucose absorption capacity) were also compared.

Experimental

Raw material

Fresh and mature northeast varieties of bhimkol banana were purchased from a local market of Tezpur, Napaam, Assam, India. For the study, sodium hydroxide and selenium dioxide were procured from Thermo Fisher Scientific India Pvt. Ltd, Mumbai. Copper sulphate, potassium sulphate, and sulfuric acid were obtained from Avantor Performance Materials India Ltd, Maharashtra. Hydrochloric acid and boric acid were supplied by Merck Specialities Private Ltd, Mumbai. Petroleum benzene was received from Merck Life Science Private Ltd, Mumbai. Hexane was obtained from Sisco Research Laboratories Pvt. Ltd, Mumbai. Further, 3,5-dinitrosalicylic acid was obtained from Loba Chemie Pvt. Ltd, Mumbai. Sodium hydrogen phosphate, sodium potassium tartrate, and glucose were supplied by Himedia Laboratories Pvt. Ltd, Maharashtra. All the chemicals were used without any further purification.

Extraction of dietary fiber from bhimkol peel using different techniques

Preparation of bhimkol peel powder. For the study, the bhimkol peel was removed from the fruit, followed by cutting the peel into small pieces using a knife. The sliced bhimkol peels were blanched using hot water bath (Make # JEIO TECH, Korea Model # BW-20G serial no. #T039511), followed by drying at 60 °C. After drying, the samples were ground and sieved to obtain bhimkol peel powders (BPP), which were then stored till further analysis. The obtained BPP was treated using hexane with solid-to-solvent ratio of 1 : 2.5 w/v for 72 h under ambient temperature to remove the fat content with slight modification to the procedure followed earlier by Wachirasiri *et al.*, 2009; Wu *et al.*, 2020.[30,31] After the treatment, hexane was evaporated using a hot air oven at 50 °C and stored for further treatment.

Ultrasonic-assisted extraction (UAE). DF was extracted from BPP using ultrasonic-assisted extraction (UAE-BPP) with a 33 kHz ultrasonic bath sonicator (Make # LABWAN, India Model # LW-UC4 serial no. #L41125). For optimizing the processing conditions, central composite design (CCD) was followed, where the independent factors were the processing time (20 to 60 min), solvent-to-solid ratio (30 to 70 mL g^{-1}), and temperature (40 to 80 °C), and one dependent variable, *viz.*, yield (%). For the study, the ultrasonic power was kept constant for all the samples (100 watt). The coded and actual values for the extraction have been represented in Table 1. The chosen solvent for the extraction was alkaline (NaOH, 1%) solution. The UAE method for the extraction of DF has been reported in several studies.[16,19,32,33] 1 g of BPP was weighed, mixed with 30 mL of NaOH solution and treated using an ultrasonic bath at 40 °C. After that, the treated sample was washed three times with distilled water, and the residue of DF was neutralized after the extraction process was completed. The treated sample was dried in a hot air oven at 50 °C, followed by grinding it using a grinder (Make # Bajaj, India Model no. #REX 500) at a normal speed to obtain a fine powder (sieve size 50 mm) and storing at room temperature till further analysis.

The extraction yield (%) of DF was measured using eqn (1).

$$Y\ (\%) = \frac{C}{W} \times 100 \quad (1)$$

where Y represents yield of the sample, C represents DF weight, and W denotes BPP weight.

Table 1 Coded and actual values for the optimization of dietary fiber extraction using CCD design[a]

		Levels		
Independent variables	Symbols	−1	0	+1
Time (min)	X_1	20	40	60
Solvent/solid ratio (mL g^{-1})	X_2	30	50	70
Temperature (°C)	X_3	40	60	80

[a] Where X_1 represents time (min), X_2 represents solvent/solid ratio (mL g^{-1}), and X_3 represents temperature (°C).

Hot water bath extraction method. The hot water bath extraction of BPP (HEM-BPP) was carried out using the method followed by Yuan *et al.*, 2019 (ref. 34) with some modification. Firstly, BPP was taken in an alkaline solution and DF was extracted using a water bath (Make # JEIO TECH, Korea Model # BW-20 G serial no. #T039511) at the optimized condition of UAE. Afterwards, the samples were processed similarly as mentioned for the UAE process.

Optimization of dietary fiber using central composite design (CCD)

CCD design was applied for optimizing DF extraction. Three independent variables such as (1) time (20 to 60 min) (X_1), (2) solvent–solid ratio (30 to 70 mL g^{-1}) (X_2), and (3) temperature (40 to 80 °C) (X_3) and one dependent variable, *viz.*, yield (%), were taken for the optimization. There were 20 experiments in CCD, including 6 centre points, 6 axial points, and 8 factorial points. The obtained experimental data were fitted into a quadratic model, as represented in eqn (2) below.

$$Y = P_0 + \sum_{i=1}^{n} P_i X_i + \sum_{i=1}^{n} P_{ii} X_i^2 + \sum_{i=1}^{n-1} \sum_{j=i=1}^{n} P_{ij} X_i X_j \quad (2)$$

where Y is yield of DF; is a constant coefficient; X_i and X_j are coded independent variables, and P_i is the linear coefficient, P_{ii} is a quadratic coefficient, P_{ij} two- factor interaction coefficient, and n is the number of independent parameters.

Characterization of dietary fiber

Physical properties

Bulk density. The bulk density (ρ bulk) of the samples (UT-BPP, HEM-BPP & UAE-BPP) was determined according to the method followed by Savlak *et al.*, 2016 (ref. 35) with minor modifications. The samples were weighed (3 g) and their volume measured using a (10 mL) graduated cylinder. The ratio of the mass of the extracted samples to the volume inside the cylinder provides the value of bulk density, as represented in the eqn (3) below.

$$\text{Bulk density } (\rho) = \frac{\text{mass of sample}}{\text{bulk volume}} \quad (3)$$

Tapped density. For measuring the tapped density, a constant volume was taken in a 10 mL graduated cylinder and a glass rod was used to tap to a constant volume.[35] The tapped density was calculated following eqn (4) below.

$$\text{Tapped density } (\rho) = \frac{\text{mass of sample}}{\text{tapped volume}} \quad (4)$$

Angle of repose. A funnel, which was placed at a certain height (2 cm), was gradually moved upwards when the samples (UT-BPP, HEM-BPP & UAE-BPP) fall on a flat surface (graph paper), forming a heap. This helped to keep the powder tip and funnel at a constant height and created a pile powder. As the powder touched the tip of the funnel, the funnel was removed and a circular mark was plotted against the perimeter of the powder heap, measuring the diameter and height of the heap, using a ruler and plotting it against the given formula (5).

$$\theta = \tan^{-1}\left(\frac{2h}{d}\right) \quad (5)$$

In the above formula, h is height (cm), and d is diameter (cm).

Density & volume. Gas pycnometry (Make # Porous Materials, inc., USA Model # PYC-100A serial no. #01262016-3269) is a non-destructive method that is used to measure the volume by the gas displacement method, which makes it perfect for determining the real density. For the analysis, samples (UT-BPP, HEM-BPP & UAE-BPP) of known weight (5 g) were sealed inside a compartment maintained at a constant temperature. The system was then filled with helium for measuring the volume and density.

Functional properties

Water holding capacity (WHC). WHC was determined according to the method used by Wang *et al.*, 2021 and Moczkowska *et al.*, 2019 (ref. 4 and 32) with minor modification. Firstly, 20 mL of distilled water was used individually to dissolve 0.5 g of the samples (UT-BPP, HEM-BPP & UAE-BPP) (W_1). The samples were kept for 24 h at the ambient temperature, after which they were centrifuged for 15 min using a centrifuge (Make # Remi Elektrotechnik Ltd, India Model # R-8C PLUS serial no. #ZILN-46961) at 6700 rpm and 25 °C. After centrifugation, the weight (W_2) was measured and the residues were immediately removed. At the end, the WHC was calculated using the following formula (6).

$$\text{WHC } (\text{g g}^{-1}) = \frac{W_2 - W_1}{W_1} \quad (6)$$

where W_2 is the pellet weight that contained the water (g) and W_1 is the weight of DF (g).

Oil holding capacity (OHC). OHC was measured by following the procedure used by Zhang *et al.*, 2017 with minor modification.[12] For the analysis, 0.5 g of the samples (UT-BPP, HEM-BPP & UAE-BPP) (W_1) were added in 5 mL of refined soybean oil and kept for 1 h at 5 °C. They were then centrifuged (Make # Remi Elektrotechnik Ltd, India Model # R-8C PLUS serial no. #ZILN-46961) at 6700 rpm for 15 min at 25 °C, followed by the removal of the sediments, and the weight (W_2) was again recorded.[4,30] OHC was determined using eqn (7).

$$\text{OHC } (\text{g g}^{-1}) = \frac{W_2 - W_1}{W_1} \quad (7)$$

where W_2 is the pellet weight containing the oil (g), and W_1 is the dry weight of DF (g).

Glucose absorption capacity. The GAC was analyzed according to the method described by Gan *et al.*, 2020; Ma & Mu 2016, Wang *et al.*, 2021, with some modifications.[4,36,37] The extracted samples (UT-BPP, HEM-BPP & UAE-BPP) (0.25 g) were mixed with 25 mL of glucose (50 and 100 mmol L^{-1}) in a centrifuge tube and was kept in an incubator (Make # Scigenics Biotech Pvt. Ltd India Model # ORBITEK LETTD serial no. #2012 400 106) at 37 °C for 6 h. After centrifuging (Make # Remi Elektrotechnik Ltd, India Model # R-8C PLUS serial no. #ZILN-46961) the samples at 4800 rpm for 10 min, 0.5 mL of the supernatant was transferred into a glass tube, where distilled

water was added to the tube until the volume reached 3 mL, followed by mixing with 2 mL of 3,5-dinitro-salicylic acid (DNS), a color development reagent. The mixture was then incubated in a water bath (Make # JEIO TECH, Korea Model # BW-20 G serial no. #T039511) at 95 °C for 10 min. After the solution temperature dropped to room temperature, it was shaken using a vortex, and the residual concentration of glucose was measured at 520 nm using a spectrophotometer (Make # Thermo Fisher Scientific Model # AQUAMATE 8100 serial no. #9A8Z246013 Verna Rd. Madison, WI 53711, USA, assembled in China) and quantified based on the standard curve.

$$\text{GAC (mmol g}^{-1}) = C_i - C_S \times V/S \quad (8)$$

In the above formula, C_i and C_S are glucose levels in supernatants before and after adsorption (mmol L^{-1}), respectively, S stands for DF (g) sample weight, while V represents the volume of glucose solution (L).

Thermal properties

Thermogravimetric analysis (TGA). Thermogravimetric analysis (TGA) of the samples (UT-BPP, UAE-BPP & HEM-BPP) was carried out using a thermogravimetric analyzer (Make # Netzsch, Germany Model # TG 209 F1 LIBRA).[19,36] For the analysis, the samples were kept in a TGA crucible and heated from 25 to 600 °C at 10 °C min^{-1} with a gas flow rate of 20 mL min^{-1} under a high-purity N_2 atmosphere.

Differential scanning calorimetry (DSC). For the DSC analysis, the DSC (Model # DSC 214 POLYMA, Make # Netzsch, Germany) apparatus was calibrated utilizing an empty aluminium pan as a point of reference. The characterization was done at a rate of 20 °C min^{-1}, a gas flow rate of 40 mL min^{-1} was selected, and the selected temperature range for the analysis was from 20 to 450 °C. An aluminium pan was filled with the sample (15 mg) and covered with an hermetically sealed aluminium lid. The peak temperature (T_p) and thermal transition (ΔH) were determined. Additionally, melting temperature, glass transition temperature, crystalline temperature, and latent and specific heats were also measured.

X-ray diffraction (XRD). An X-ray diffractometer operated with Cu radiation at 40 kV/125 mA of incident current was used to perform X-ray diffraction (Make # BRUKER, Germany Model # D8 FOCUS) of the samples. An angle of diffraction between 10° and 80° was selected for the characterization with a step size of 0.5°. The crystallinity index (CI) of the DF samples was obtained using the diffraction intensity data in accordance with Ma & Mu 2016; Gan *et al.*, 2020.[36,37]

Fourier transform infrared (FTIR) spectroscopy. For the analysis, the extracted DFs were thoroughly mixed with KBr in a ratio of 1 : 3 and pelletized. The FTIR spectra of the DFs obtained by three different extraction methods (UT-BPP, UAE-BPP & HEM-BPP) were recorded using an FTIR spectrometer (Make # BRUKER, Germany Model # D8 FOCUS) in the wavelength range from 400 to 4000 cm^{-1} with 32 scans and a resolution of 4 cm.

Statistical analysis

The statistical analysis was performed using the Design Expert software version 13. The mean ± standard deviation (SD) of three parallel measurements was used to represent the results, and a significance level of $p < 0.05$ was used to evaluate mean differences using analysis of variance (ANOVA) polynomial quadratic regression model.

Results and discussion

Proximate compositions of bhimkol peel powder

The agro-industrial waste bhimkol peel is considered to be a remarkable resource of DF.[38,39] The BPP obtained after cutting, blanching, drying, and sieving was analyzed for the proximate composition as represented in Table 2. The crude fiber content of BPP was found to be around 23.39 ± 1.10%, which is found to be in line with the results from banana peel (19.0%) as reported by Pyar & Peh 2018.[38] Additionally, the other proximate compositions of BPP were found as 7.30%, 2.22%, 1.40%, and 10.47% for protein, fat, moisture content, and ash content, respectively. Similar proximate compositions of banana peels have previously been reported in several research study.[30,40,41] Considering this, bhimkol peels are a good resource of crude fiber. Further, the various extraction techniques are employed to extract DF from BPP such as UAE, and hot water bath extraction.

Optimization of extraction of dietary fiber from bhimkol peel powder

The optimization of processing conditions to extract bhimkol (*Musa balbisiana*) peel powder (BPP)-based DF was done using response surface methodology. The factors and level of the central composite design (CCD) for the extraction such as independent variables including time (20 to 60 min) (X_1), solvent–solid ratio (30 to 70 mL g^{-1}) (X_2), and temperature (40 to 80 °C) (X_3) and one dependent variable such as yield (%) have been represented in Fig. 1 and Table 3. The entire experimental design representing the actual, predicted value, and coded values of the independent variables along with the obtained yield of DF factors has been represented in Fig. 2 and Table 3.

Various processing conditions such as time, solvent-to-solid ratio, and processing temperature influence the yield of DF from BPP. Furthermore, the processing time influences the yield of DF and if the extraction time increases, it may cause thermal degradation in the DF. Based on the responses, the highest processing time for extracting DF was 60 min. In the present study, the extraction process was carried out at different times (20, 40, and 60 min), and the highest yield was obtained at

Table 2 Proximate properties of bhimkol peel powder

Properties	Content[a] (%)
Moisture content	1.40 ± 0.06
Fat	2.22 ± 0.09
Protein	7.30 ± 0.25
Crude fiber	23.39 ± 1.10
Ash	10.47 ± 0.45

[a] Different proximate compositions are represented as average with standard deviation.

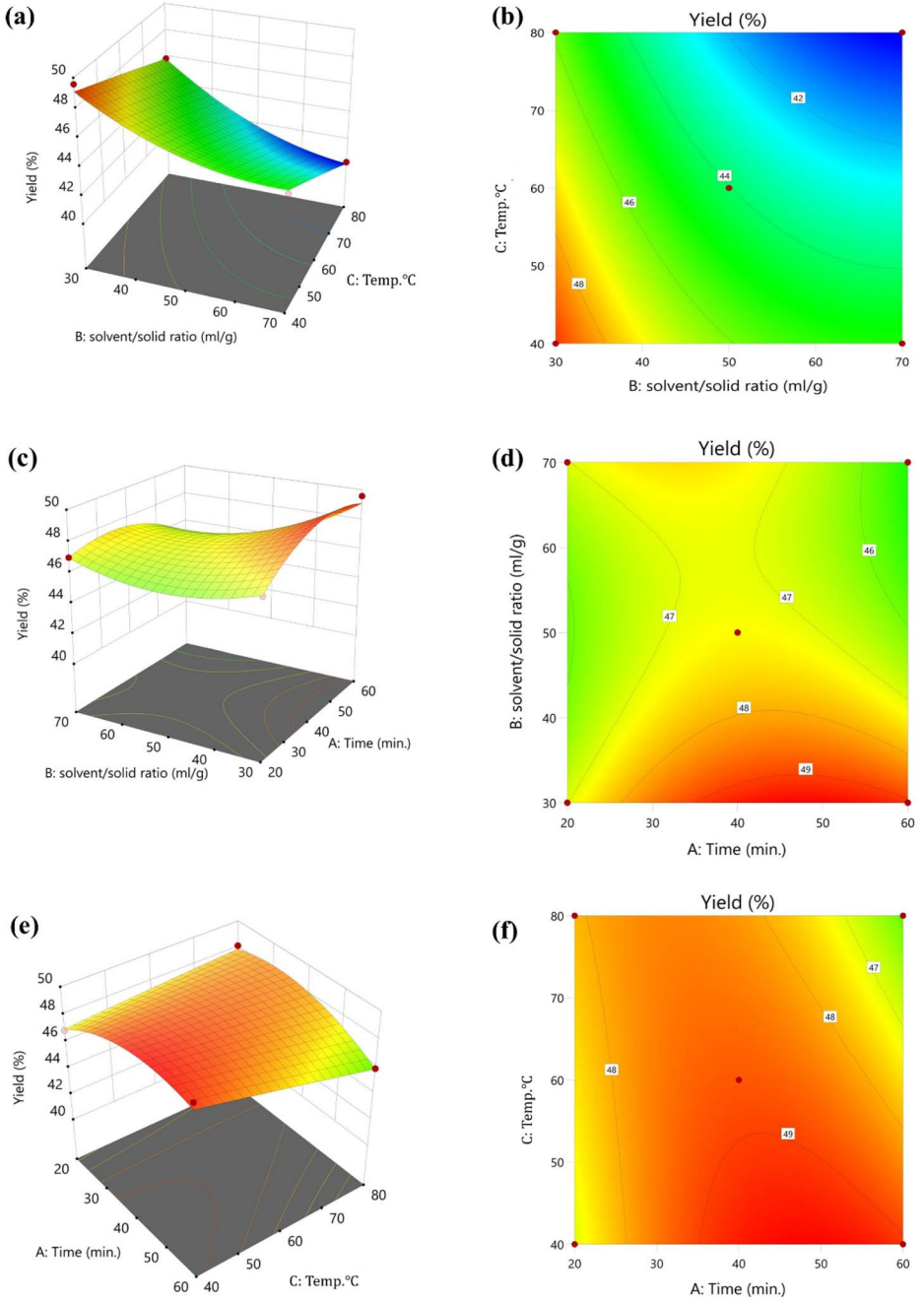

Fig. 1 Effect of optimization of independent variables for the 3D graph: (a) extraction time, (c) extraction temperature, (e) solvent/solid ratio, and for 2D graph (b) extraction time, (d) extraction temperature, and (f) solvent/solid ratio on the extraction yield of DF.

60 min, as shown in Fig. 1a and b. The effect of temperature on the DF yield was determined in the range from 40 to 80 °C. The highest yield of DF was obtained at 40 °C, and the lowest yield was obtained at the highest selected temperatures. According to the study conducted by Zhang *et al.*, 2017,[12] the yield of DF increased at 1% NaOH concentration, and temperature also plays a significant role in determining the optimum DF production temperature at 40 °C (Fig. 1c and d). Furthermore, a subsequent increase in temperature resulted in a rapid reduction in the yield of DF from 49.58 ± 0.88% to 40.25 ± 2.01%. The yield of DF was also increased at solvent/solid ratio of 30 : 1, as shown in Fig. 1e and f; similar trends have been observed in the research reported by Sun *et al.* 2018.[25] Considering this, as represented in Table 4, the results of 20 experiments obtained using a CCD design of RSM to optimize the processing conditions have been represented. The outcomes of single factor experiments were used as basis for these investigations. Polynomial regression model analysis and significance test were done to study the interaction of various independent variables on the yield (Table 4). The extraction yield can be explained by the following quadratic regression model represented in eqn (9).

Table 3 Variables for central composite design and responses for dietary fiber extraction

	Coded variable levels			Yield[a] (%)	
Run	Factor 1 *A*: time (min)	Factor 2 *B*: solvent/solid ratio (mL g^{-1})	Factor 3 *C*: temperature (°C)	Actual value	Predicated value
1	40 (0.00)	50 (0.00)	60 (0.00)	46.60 ± 1.56	46.28
2	40 (0.00)	30 (−1.00)	60 (0.00)	48.09 ± 0.53	48.79
3	20 (−1.00)	50 (0.00)	60 (0.00)	46.16 ± 0.14	45.93
4	40 (0.00)	50 (0.00)	60 (0.00)	46.12 ± 1.02	46.28
5	40 (0.00)	50 (0.00)	60 (0.00)	45.45 ± 0.48	46.28
6	60 (1.00)	30 (−1.00)	80 (1.00)	45.91 ± 0.76	45.88
7	60 (1.00)	30 (−1.00)	40 (−1.00)	49.58 ± 0.88	49.09
8	40 (0.00)	70 (1.00)	60 (0.00)	46.44 ± 1.19	45.92
9	20 (−1.00)	30 (−1.00)	40 (−1.00)	46.91 ± 0.88	46.98
10	40 (0.00)	50 (0.00)	40 (−1.00)	47.05 ± 0.41	47.27
11	60 (1.00)	70 (1.00)	80 (1.00)	40.25 ± 2.01	40.14
12	20 (−1.00)	30 (−1.00)	80 (1.00)	48.15 ± 0.22	47.89
13	40 (0.00)	50 (0.00)	60 (0.00)	46.51 ± 0.69	46.28
14	40 (0.00)	50 (0.00)	60 (0.00)	46.65 ± 1.07	46.28
15	20 (−1.00)	70 (1.00)	80 (1.00)	45.61 ± 0.05	46.05
16	40 (0.00)	50 (0.00)	60 (0.00)	46.68 ± 1.05	46.28
17	60 (1.00)	70 (1.00)	40 (−1.00)	44.97 ± 1.62	45.18
18	40 (0.00)	50 (0.00)	80 (1.00)	45.25 ± 1.09	45.21
19	20 (−1.00)	70 (1.00)	40 (−1.00)	46.99 ± 0.05	46.97
20	60 (1.00)	50 (0.00)	60 (0.00)	43.62 ± 1.54	44.03

[a] Mean = 3 ± standard deviation.

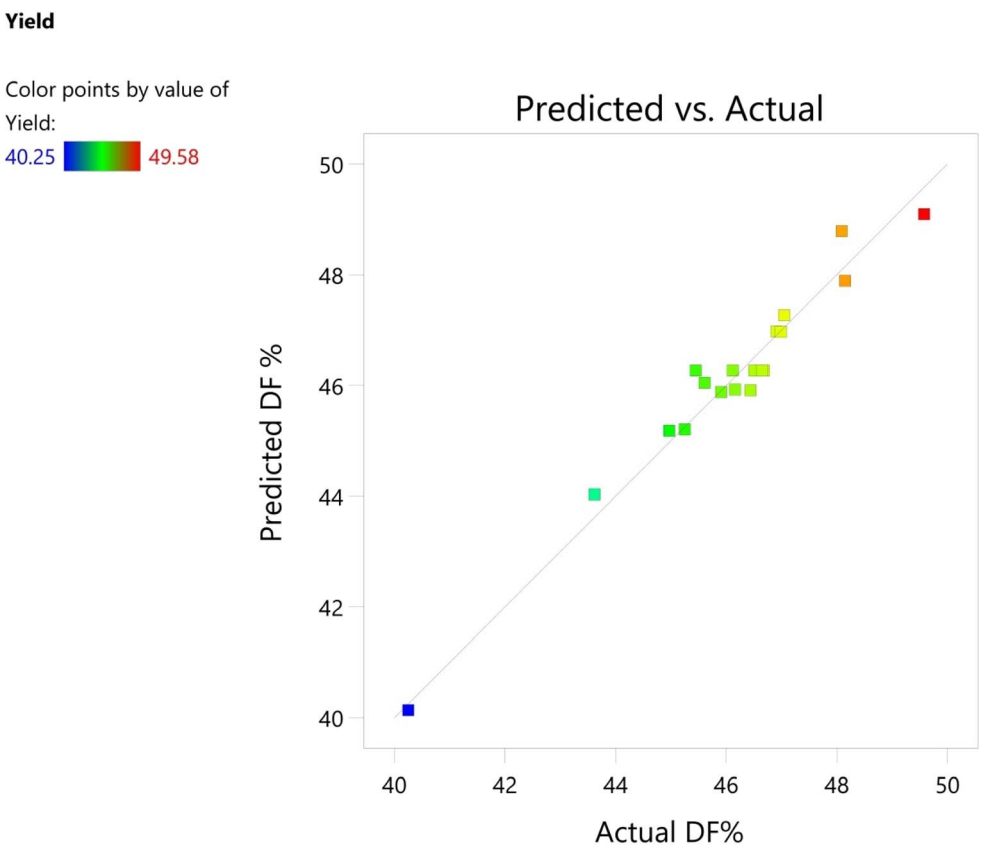

Fig. 2 Effect of optimization of independent variables (actual and predicted value) on the extraction yield of DF.

Table 4 Significance of the regression equation coefficients (quadratic model ANOVA)[a,b]

Source	Sum of squares	DF	MSS	*F*-Value	*P*-Value	
Model	64.05	9	7.12	25.68	<0.0001	**Significant**
A-Time (X_1)	9.01	1	9.01	32.49	0.0002	
B-Solvent/solid ratio (X_2)	20.68	1	20.68	74.61	<0.0001	
C-Temp. (X_3)	10.67	1	10.67	38.50	0.0001	
AB (X_1X_2)	7.62	1	7.62	27.51	0.0004	
AC (X_1X_3)	8.51	1	8.51	30.70	0.0002	
BC (X_2X_3)	1.68	1	1.68	6.07	0.0334	
A^2	4.62	1	4.62	16.65	0.0022	
B^2	3.20	1	3.20	11.56	0.0068	
C^2	0.0035	1	0.0035	0.0125	0.9133	
Residual	2.77	10	0.2772			
Lack of fit	1.62	5	0.3246	1.41	0.3568	**Not significant**
Pure error	1.15	5	0.2297			
Cor total	66.82	19				

[a] $R^2 = 0.9585$, adjusted $R^2 = 0.9212$, predicated $R^2 = 0.7213$, CV% = 1.14, adequate precision = 24.0604. [b] df, degrees of freedom; MSS, mean sum of square, CV = coefficient of variation.

$$Y = 42.19 + 0.52X_1 - 0.21X_2 + 0.11X_3 - 0.002X_1X_2 - 0.002X_1X_3 - 0.0009X_2X_3 - 0.003{X_1}^2 + 0.003{X_2}^2 - 0.0001{X_3}^2 \quad (9)$$

The results of ANOVA that was used to determine and sum up the effects of significant variables in both quadratic forms and linear are compiled in Table 4. The model has a *P*-value of <0.0001 and an *F*-value of 25.68. Further, the ANOVA quadratic regression model ($p < 0.0001$) and the R^2 value (0.9585) were significant in the extraction of DF. The lack-of-fit was non-significant ($p > 0.05$), indicating that the yield of DF can be accurately predicted using the quadratic model. In this case, the coefficients X_1, X_2, X_3, X_1X_2, X_1X_3, X_2X_3, ${X_1}^2$, and ${X_2}^2$ were found to be significant model terms, and the other coefficients were insignificant ($p > 0.05$).

The lack-of-fit was not significant relative to the pure error because the corresponding *F*-value was 1.41. In addition, the value of the determination coefficient (R^2) was 0.9585, which implies that 95.85% of the variation could be explained by the model. The relatively low values of the coefficient of variation (1.14%) and adequate precision (24.0604) indicate a good model fit.

Extraction of dietary fiber using UAE and hot water extraction method

In this research, the yield of extraction of DF from BPP was compared using two different methods such as UAE and hot water bath extraction method (HEM). The highest yield of DF obtained using the UAE method was 49.19 ± 1.39%, whereas for the HEM method, it was 45.54 ± 2.32%. The highest yield of DF by the ultrasonic bath method was obtained due to the involved frequency of the ultrasonication, which resulted in the break-down of the cell wall of the sample to extract DF, leading to the increased yield of DF when compared to HEM.[12,25] Additionally, the temperature also influenced the yield of DF along with the frequency of ultrasonication.[12]

Physical properties. The observed physical properties of BPP in terms of bulk density, tapped density, angle of repose, density, and volume have been represented in Table 5. The lowest bulk density was obtained for UAE-BPP (0.31 ± 0.03 g mL^{-1}), while the highest value was obtained for untreated BPP (0.55 ± 0.02 g mL^{-1}). The bulk density value increases when the particle size of the powder decreases.[42] Additionally, the higher tapped density was found for untreated BPP (0.69 ± 0.03 g mL^{-1}) and the lowest value was for UAE-BPP (0.38 ± 0.01 g mL^{-1}). The repose ranges of BPP were from 29.62 to 32.93°, in which lowest value was 29.62° ± 1.29 for UAE-BPP and the highest value was 32.93° ± 1.49 for HEM-BPP. The results are similar for all the properties according to Anuar *et al.*, 2019.[43] The value of density (1.66 ± 0.01 g cm^{-3}) for UT-BPP was higher compared to that of HEM-BPP (1.55 ± 0.01 g cm^{-3}). The UT-BPP samples have higher value, meaning that they occupy less area during storage. The higher density is corresponding to lower porosity. The value of volume ranges from 1.84 to 1.91 cm^3, where a lower value of volume was obtained at UT-BPP (1.84 ±

Table 5 Physical properties of extracted BPP dietary fiber

Properties	UT-BPP	HEM-BPP	UAE-BPP
Bulk density (g mL^{-1})	0.55 ± 0.02^a	0.39 ± 0.01^b	0.31 ± 0.03^c
Tapped density (g mL^{-1})	0.69 ± 0.03^a	0.5 ± 0.02^b	0.38 ± 0.01^c
Angle of repose (°)	$31.95 \pm 1.46^{a,b}$	32.93 ± 1.49^a	29.62 ± 1.29^c
Density (g cm^{-3})	1.61 ± 0.01^a	1.55 ± 0.01^c	1.57 ± 0.01^b
Volume (cm^3)	1.84 ± 0.01^b	1.91 ± 0.01^a	1.91 ± 0.01^a

Data sets are represented as mean ± SD. Different letters (*a*, *b*, *c*) define the significant differences between samples ($p < 0.05$).

0.01) and both the treated samples had similar results (1.91 ± 0.01).

Hydration and functional properties. The hydration and functional properties (WHC, OHC, and GAC) of BPP have been addressed in this section. A moist material's water holding capacity (WHC) is determined when it is compressed or centrifugal gravitational force is applied. This includes connected, hydrodynamic, and physically trapped water. WHC is influenced by the surface areas, densities, and structures of DF along with the hydrophilic nature, chemical composition and amount.[4] The WHC value of BPP DF samples ranged from 6.67 to 9.41 g g^{-1}, as shown in Fig. 3a. The highest value of WHC was found in UAE-BPP (9.41 ± 0.35 g g^{-1}), while the lowest value of WHC was observed in UT-BPP (6.67 ± 0.31 g g^{-1}). The ultrasonic extraction of the DF sample was increased for WHC compared to the other extraction methods, and similar results were reported by Karaman *et al.*, 2017.[5]

The DF for OHC play a critical role in food applications like reducing fat loss during cooking or removing excess fat from human body.[4,12] OHC depends on the hydrocolloid, surface properties, hydrophobic characteristics and total electrical charge density.[4,44] BPP-based DF has an OHC value ranging from 1.84 to 2.72 g g^{-1}. As shown in Fig. 3a, HEM-BPP had higher ability to retain oil (2.71 ± 0.11 g g^{-1}), whereas DF obtained by UT-BPP has an OHC of 1.84 ± 0.07 g g^{-1}. According to SEM, the partially soft texture produced by ultrasonic treatment may be the source of the higher OHC of BPP-DF.

Additionally, the digestive juice contains DF, which binds to glucose, lowering postprandial blood glucose. Consequently, another major functional characteristic of DF is GAC. As shown in Fig. 3b, we found that samples of DF had a significant effect on glucose binding at different glucose concentrations of 50 mmol g^{-1} and 100 mmol g^{-1} and depends upon how the glucose solution will bind with the sample and its reaction.

The GAC glucose concentration of UT-BPP-based DF at 100 mmol g^{-1} concentration was found to be higher than that at 50 mmol g^{-1} concentration, as shown in Fig. 3b. Wang *et al.*, 2021 observed that IDF absorbs more glucose as compared to SDF.[4] This finding suggest that DF extraction methods may have an impact on GAC.

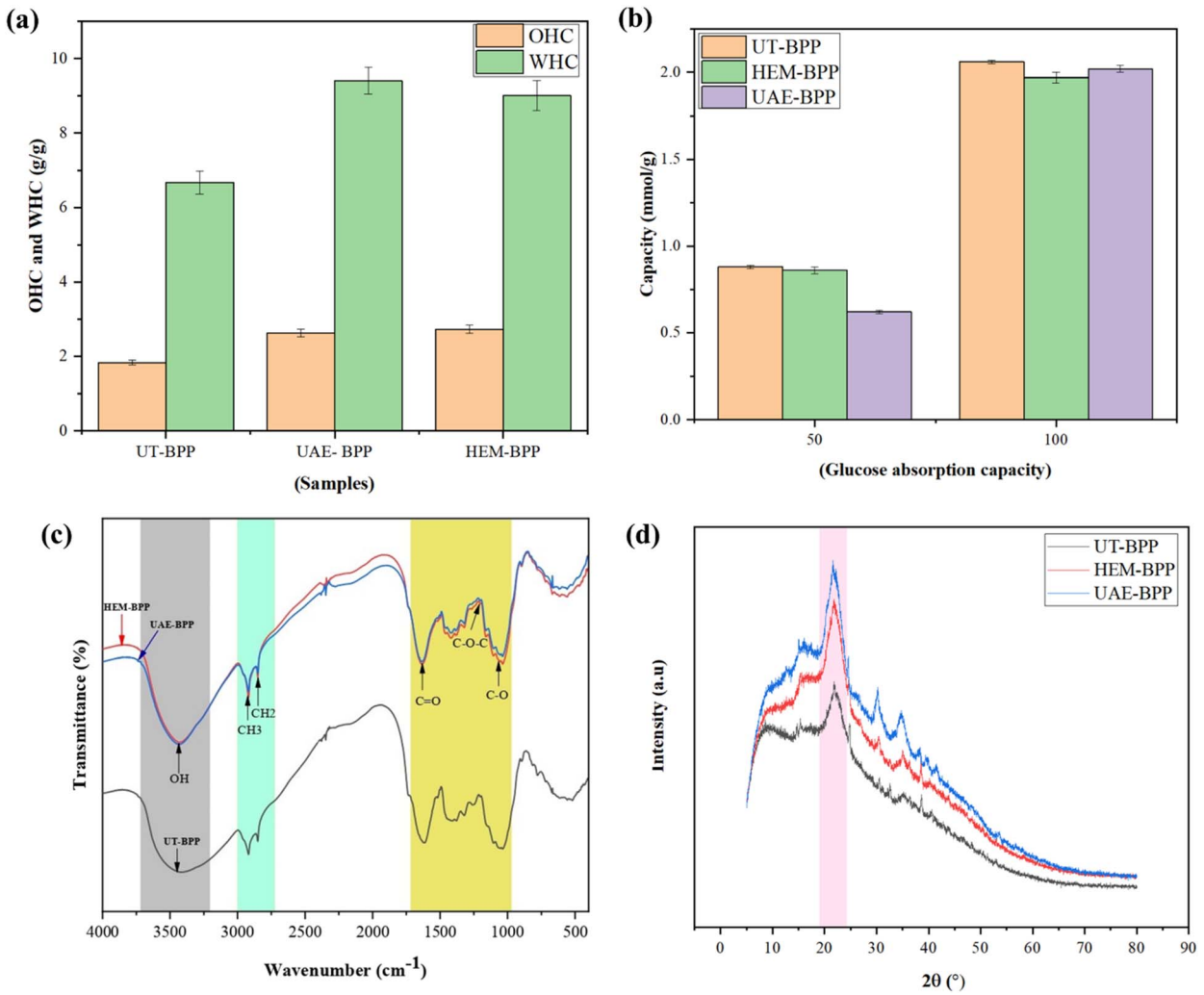

Fig. 3 Hydration and functional properties of BPP dietary fiber: (a) oil holding capacity and water holding capacity, (b) glucose absorption capacity, (c) FTIR spectra, and (d) XRD patterns.

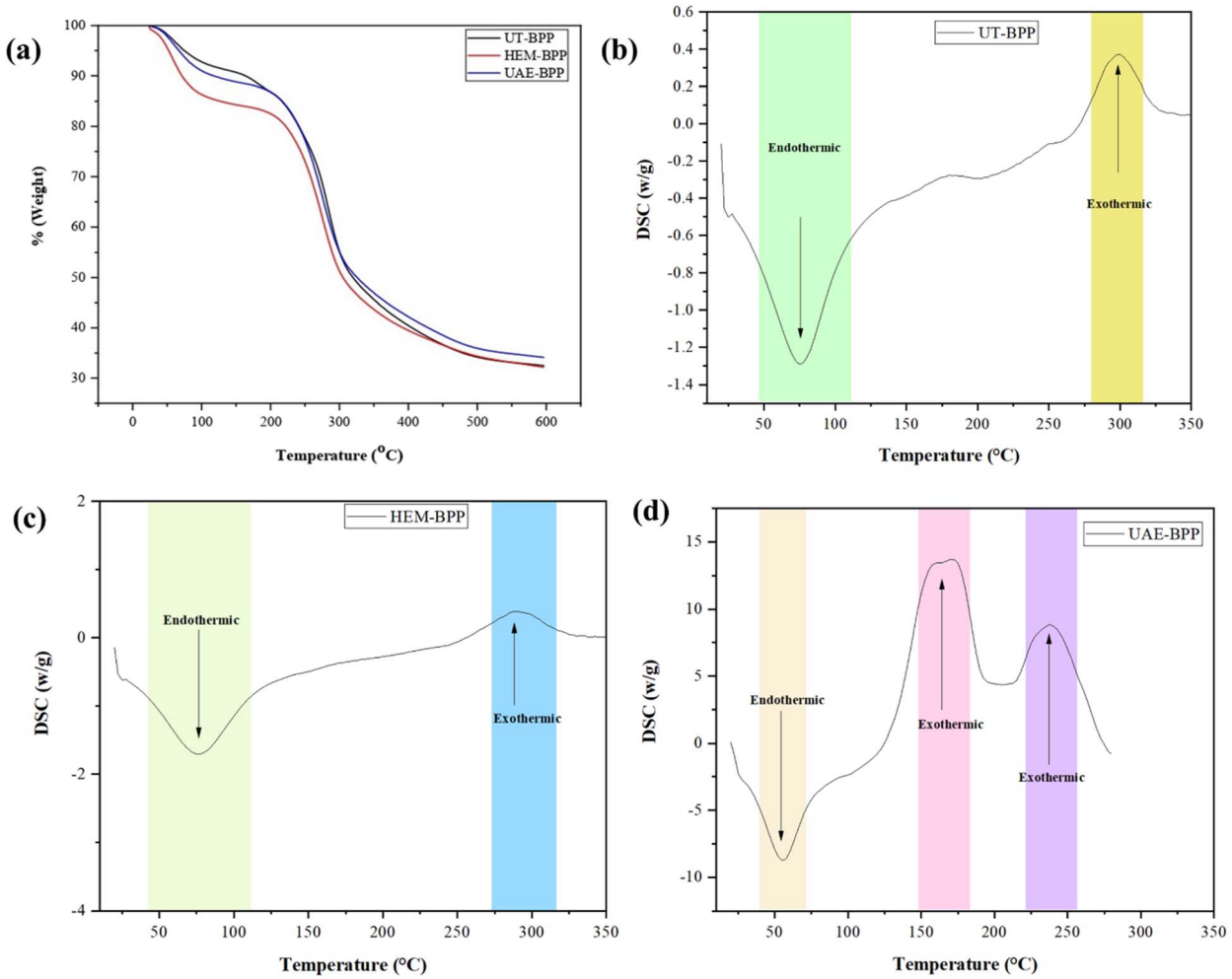

Fig. 4 (a) Thermogravimetric and differential scanning calorimetry curves of BPP dietary fiber: (b) UT-BPP, (c) HEM-BPP, and (d) UAE-BPP.

Fourier transform infrared (FT-IR) spectroscopy. FTIR spectroscopy was carried out to analyze the spectroscopic features of BPP DF in different samples such as UT-BPP, HEM-BPP and UAE-BPP, as shown in Fig. 3c. The results were obtained using the polysaccharide components, namely, cellulose, hemicellulose, and lignin. The peaks located between 3000 and 2800 cm^{-1} are attributed to the CH stretching band because polysaccharides include methyl or methylene groups of cellulose.[12,32,45] It has been observed that the stretching vibration of CH on the sugar's methyl and methylene group absorption is represented by the wide peak at 2921 cm^{-1} and 2851 cm^{-1}, while the absorption broad peak for the OH group is at 3444 cm^{-1}; similar results were reported by Wang *et al.*, 2021 and Zhang *et al.*, 2017.[4,12] These absorption peaks are typical polysaccharide absorption peaks from DF because of the variable angle vibration of CH between 1200 and 1500 cm^{-1}, according to Wang *et al.*, 2022.[46] The stretching vibration and deformation of the peak at 1636 cm^{-1} for the carbonyl group (C═O) might be the characteristic asymmetric and symmetric absorption; similar results were obtained by Gan *et al.*, 2020.[36] The C–O stretching vibration, which may be the bending vibration of primary alcohols or C–O–C and C–O, was specifically responsible for the distribution of peaks at 1230–1040 cm^{-1}. The ether stretching vibration peak is at 1205 cm^{-1} for C–O–C, and the C–O peak is at the 1063 cm^{-1}.[24]

X-ray diffraction. The crystallinity changes were evaluated by XRD, which determine the aggregation status of DF molecules. A strong diffraction peak was observed for UT-BPP, HEM-BPP and UAE-BPP, as shown in Fig. 3d. The characteristic XRD peaks were observed at 2θ of 21.79°, 21.94°, and 21.61° for UT-BPP, HEM-BPP, and UAE-BPP respectively. The obtained crystallinity for UT-BPP, HEM-BPP, and UAE-BPP were 23.5%, 22.69%, and 26.78%, respectively. The crystallinity obtained for HEM-BPP and UT-BPP is lower than that of UAE-BPP, suggesting that ultrasonic treatment may reduce the degree of soluble DF polymerization and increase swelling, solubility and ability

Table 6 Thermogravimetric analysis data for dietary fiber extracted using, UT-BPP, HEM-BPP, and UAE-BPP

Samples	T_{10} (°C)	T_{50} (°C)
UT-BPP	162.30	317.26
HEM-BPP	69.75	304.74
UAE-BPP	117.30	324.78

Table 7 Differential scanning calorimetry data of dietary fiber extracted using, UT-BPP, HEM-BPP, and UAE-BPP

	Endothermic reaction			Exothermic reaction		
Sample	Onset (°C)	Peak (°C)	End set (°C)	Onset (°C)	Peak (°C)	End set (°C)
UT-BPP	43.7	74.9	111.8	268.2	300.3	323.1
HEM-BPP	42.8	76.6	115.0	249.9	290.0	332.0
UAE-BPP	57.2	96.5	134.8	250.0	327.1	365.6

to hold water and oil. A similar result was observed by Zhang *et al.*, 2017.[12]

Thermal properties

Thermogravimetric analysis (TGA). The thermal analysis of BPP-based DF was performed by TGA with slight modification. Thermal stability is an essential property of polymers used in edible packaging.[12] Thermogravimetric analysis data of DF extracted using UT-BPP, HEM-BPP, and UAE-BPP have been represented in Fig. 4a and Table 6. The curves of DF have been classified in three stages, where the first stage is from 35 to 203 °C and includes weight loss due to the evaporation of water from the samples. The mass loss for UT-BPP, HEM-BPP, and UAE-BPP was 12.76%, 15.89%, and 11.41%, respectively. A higher weight loss is found in the second stage (215–450 °C), where the mass loss was 47.85%, 44.02%, and 46.7% for UT-BPP, HEM-BPP, and UAE-BPP, respectively. The third stage is 485–600 °C, and the residual mass of the samples is 1.84%, 2.39%, and 2.11%. Additionally, the temperature for 10% (T_{10} °C) and 50% (T_{50} °C) loss in weight during the TGA analysis of the samples has been represented in Table 6. It has been observed that UAE-BPP significantly improved the thermal stability compared to HEM-BPP. It has also been observed that the sample weight loss slowed down in the last stage, which may have been caused by the char thermal decomposition.

Differential scanning calorimetry. A DSC analysis was carried out to provide details about the endothermic and exothermic reactions. The properties of DF in terms of onset, peak and endpoint temperatures are shown in Fig. 4b–d and Table 7. Additionally, two peaks were visible in the endothermic range (42–135 °C) and exothermic range (249–360 °C) of the DSC curve, which were in line with those reported by Karaman *et al.*, 2017.[5] In this study, it has been found that the endothermic peak shifts were found to change from 43.7 to 57.2 °C for onset, 74.9 to 96.5 °C for peak and end set temperature from 111.8 to 134.8 °C. The exothermic peaks were found to change for the onset temperature from 249.9 to 268.2 °C, peak temperature from 290.0 to 327.1 °C, and end set temperature from 323.1 to 365.6 °C for the samples.[12,33] The exothermic peaks in the DSC curve indicate the ongoing oxidation and thermal breakdown, which also includes the vaporization and loss of volatile compounds. The random break of glycosidic linkages is followed by a more thorough breakdown and here, the pyrolysis of polysaccharides starts.[47] The second peak from 225 to 260 °C is for the in UAE-treated sample, where DF may involve structural changes as a result of ultrasound treatment, particularly the breakdown of some crystalline areas and the recrystallization process.[48]

Conclusions

In this study, the optimization of DF extraction from BPP using the UAE method was done through RSM (CCD). The extracted DF was analyzed for its physicochemical, hydration, functional, and thermal properties and compared with the conventional extraction method. The results show that using an alkaline solvent for UAE gave a higher yield of DF (49.19%) compared to the hot water extraction method (45.54%). UAE-based DF extraction methods often yield DF with superior properties compared to traditional hot water extraction. Furthermore, the DF extracted using UAE-BPP exhibited enhanced WHC, OHC, crystallinity, and thermal properties, indicating improved functional properties. The obtained DF can be utilized in food sectors, such as in bakery, dairy products, and processed foods for improved food properties and qualities.

Data availability

The data can be obtained upon request to the authors.

Author contributions

Laxmikant Rawat: original draft writing, review and editing. Tabli Ghosh: conceptualization, supervision, validation, final review and editing.

Conflicts of interest

The authors declare no conflict of interest related to this research.

Acknowledgements

The authors are thankful to the Sustainable Food Lab at the Department of Food Engineering and Technology, School of Engineering, Tezpur University, Assam, India, for the funding.

References

1 T. Ghosh and K. K. Dash, *Engineering in Agriculture, Environment and Food*, 2018, **11**, 186–195.
2 M. B. Gogoi, I. Chetia, B. K. Sarmah, T. Nath, S. Bhowal, K. Dey and P. Bhorali, *Int. J. Curr. Microbiol. Appl. Sci.*, 2020, **9**, 2555–2565.
3 R. B. Watharkar, S. Chakraborty, P. P. Srivastav and B. Srivastava, *J. Food Meas. Char.*, 2021, **15**, 3336–3349.

4 K. Wang, M. Li, Y. Wang, Z. Liu and Y. Ni, *Food Hydrocolloids*, 2021, **110**, 106162.
5 E. Karaman, E. Yılmaz and N. B. Tuncel, *Bioact. Carbohydr. Diet. Fibre*, 2017, **11**, 9–17.
6 L. Cheng, X. Zhang, Y. Hong, Z. Li, C. Li and Z. Gu, *Int. J. Biol. Macromol.*, 2017, **101**, 1004–1011.
7 K. S. Poutanen, S. Fiszman, C. F. Marsaux, S. P. Pentikainen, R. E. Steinert and D. J. Mela, *Am. J. Clin. Nutr.*, 2018, **108**, 437–444.
8 L. R. Ferguson, R. R. Chavan and P. J. Harris, *Nutr. Cancer*, 2001, **39**, 155–169.
9 A. Kurhade, S. Patil, S. K. Sonawane, J. S. Waghmare and S. S. Arya, *J. Food Meas. Char.*, 2016, **10**, 32–41.
10 Y. A. McKenzie, R. K. Bowyer, H. Leach, P. Gulia, J. Horobin, N. A. O'Sullivan and IBS Dietetic Guideline Review Group on behalf of Gastroenterology Specialist Group of the British Dietetic Association, *J. Hum. Nutr. Diet.*, 2016, **29**, 549–575.
11 A. Ren, L. Chen, W. Zhao, S. Shan, Z. Li and Z. Tang, *J. Funct. Foods*, 2023, **107**, 105659.
12 W. Zhang, G. Zeng, Y. Pan, W. Chen, W. Huang, H. Chen and Y. Li, *Carbohydr. Polym.*, 2017, **172**, 102–112.
13 Y. A. Begum and S. C. Deka, *J. Food Process. Preserv.*, 2019, **43**, e14256.
14 V. V. Khanpit, S. P. Tajane and S. A. Mandavgane, *Biomass Convers. Biorefin.*, 2021, 1–20.
15 D. Dhingra, M. Michael, H. Rajput and R. T. Patil, *J. Food Sci. Technol.*, 2012, **49**, 255–266.
16 Q. Ma, W. Wang, Z. Ma, Y. Liu, J. Mu, J. Wang and X. Hui, *J. Funct. Foods*, 2021, **84**, 104606.
17 X. Du, L. Wang, X. Huang, H. Jing, X. Ye, W. Gao and H. Wang, *LWT*, 2021, **143**, 111031.
18 E. Perez-Lopez, I. Mateos-Aparicio and P. Ruperez, *J. Food Sci. Technol.*, 2017, **54**, 1333–1339.
19 B. Kaur, P. S. Panesar and A. Thakur, *Biomass Convers. Biorefin.*, 2021, 1–10.
20 I. Buljeta, D. Subaric, J. Babic, A. Pichler, J. Simunovic and M. Kopjar, *Appl. Sci.*, 2023, **13**, 9309.
21 Y. Y. Yang, S. Ma, X. X. Wang and X. L. Zheng, *J. Chem.*, 2017, 9340427.
22 V. Tejada-Ortigoza, T. Garcia-Cayuela, J. Welti-Chanes, M. P. Cano and J. A. Torres, *Science and Technology of Fibers in Food Systems*, 2020, pp. 363–381.
23 H. Fooladi, S. A. Mortazavi, A. Rajaei, D. Salar Bashi and S. Savabi Sani Kargar, *Optimize the extraction of phenolic compounds of jujube (Ziziphus Jujube) using ultrasound-assisted extraction method*, 2013, **https://d1wqtxts1xzle7.cloudfront.net/77283724/271_1-libre.pdf?1640368532=&response-contentdisposition=inline%3B+filename%3DOptimize_the_extraction_of_phenolic_comp.pdf&Expires=1730182109&Signature=C4Sbpr9c58bX5v4ARYimUOwhZgzpjmM0W9umUApJJ4xeE4bAT5nSuLfImXlo4C0XgtBzhqvlp7jj-B1sZxSe4NGyz261YupZyU23u0kSjt3R7BrhFjc46VsB4YZhQePvtVElPIIBOwejNFoVvvUEf6VkouC3BoqaT62mnUHcB4jhqfB4jFb1XjdE83UqQ__&Key-Pair-Id=APKAJLOHF5GGSLRBV4ZA**.
24 C. Chen, L. J. You, A. M. Abbasi, X. Fu and R. H. Liu, *Carbohydr. Polym.*, 2015, **130**, 122–132.
25 J. Sun, Z. Zhang, F. Xiao, Q. Wei and Z. Jing, *IOP Conf. Ser.: Mater. Sci. Eng.*, 2018, **392**, 052005.
26 S. Adapa, H. Dingeldein, K. A. Schmidt and T. J. Herald, *J. Dairy Sci.*, 2000, **83**, 2224–2229.
27 Y. Niu, N. Li, Q. Xia, Y. Hou and G. Xu, *LWT*, 2018, **88**, 56–63.
28 N. Aravind, M. Sissons and C. M. Fellows, *Food Chem.*, 2012, **131**, 893–900.
29 S. Martinez-Cervera, A. Salvador, B. Muguerza, L. Moulay and S. M. Fiszman, *LWT*, 2011, **44**, 729–736.
30 P. Wachirasiri, S. Julakarangka and S. Wanlapa, *Songklanakarin J. Sci. Technol.*, 2009, **31**, 605–611.
31 C. Wu, F. Teng, D. J. McClements, S. Zhang, Y. Li and Z. Wang, *Food Res. Int.*, 2020, **134**, 109251.
32 M. Moczkowska, S. Karp, Y. Niu and M. A. Kurek, *Food Hydrocolloids*, 2019, **90**, 105–112.
33 M. A. Kurek, S. Karp, J. Wyrwisz and Y. Niu, *Food Hydrocolloids*, 2018, **85**, 321–330.
34 Q. Yuan, S. Lin, Y. Fu, X. R. Nie, W. Liu, Y. Su and D. T. Wu, *Int. J. Biol. Macromol.*, 2019, **127**, 178–186.
35 N. Savlak, B. Turker and N. Yeşilkanat, *Food Chem.*, 2016, **213**, 180–186.
36 J. Gan, Z. Huang, Q. Yu, G. Peng, Y. Chen, J. Xie and M. Xie, *Food Hydrocolloids*, 2020, **101**, 105549.
37 M. M. Ma and T. H. Mu, *Food Chem.*, 2016, **194**, 237–246.
38 H. Pyar and K. K. Peh, *Res. J. Chem. Environ.*, 2018, **22**, 108–111.
39 M. K. Saeed, N. Zahra, A. Saeed, S. Y. E. D. Quratulain and S. H. I. ABIDI, *Acta Pharm. Sci.*, 2024, **62**, 89–103.
40 E. H. Lee, H. J. Yeom, M. S. Ha and D. H. Bae, *Food Sci. Biotechnol.*, 2010, **19**, 449–455.
41 A. N. Tsado, N. R. Okoli, A. G. Jiya, D. Gana, B. Saidu, R. Zubairu and I. Z. Salihu, *BIOMED Natural and Applied Science*, 2021, **1**, 032–042.
42 J. Ahmed, A. Taher, M. Z. Mulla, A. Al-Hazza and G. Luciano, *J. Food Eng.*, 6186, **201**, 34–41.
43 M. S. Anuar, S. M. Tahir, M. I. Najeeb and S. B. Ahmad, *Adv. Mater. Processes Technol.*, 2019, **5**, 181–190.
44 M. Jia, J. Chen, X. Liu, M. Xie, S. Nie, Y. Chen and Q. Yu, *Food Hydrocolloids*, 2019, **94**, 468–474.
45 M. C. Rouhou, S. Abdelmoumen, S. Thomas, H. Attia and D. Ghorbel, *Int. J. Biol. Macromol.*, 2018, **116**, 901–910.
46 S. Wang, Y. Fang, Y. Xu, B. Zhu, J. Piao, L. Zhu and J. Wu, *J. Funct. Foods*, 2022, **93**, 105081.
47 D. Mudgil, S. Barak and B. S. Khatkar, *Int. J. Biol. Macromol.*, 2012, **50**, 1035–1039.
48 Y. Wang, W. Wang, Y. Wu, J. JiLiu, X. Hu, M. Wei and L. Cao, *Front. Nutr.*, 2023, **10**, 1157015.